Cu(In,Ga)Se$_2$ surface treatment with Na and NaF:

A combined photoelectron spectroscopy and surface photovoltage study in ultra-high vacuum

V. Parvan[1], A. Mizrak[1], I. Majumdar[1], B. Ümsür[1], W. Calvet[1,a)], D. Greiner[1],
C. A. Kaufmann[1], T. Dittrich[2,b)], E. Avancini[1,c)] I. Lauermann[1,d)]

[1] *PVcomB, Helmholtz-Zentrum Berlin für Materialien and Energie GmbH, Schwarzschildstr. 3, 12489 Berlin, Germany*

[2] *Institut für Siliziumphotovoltaik, Helmholtz-Zentrum Berlin für Materialien and Energie GmbH, Kekuléstr. 5, 12489 Berlin, Germany*

Abstract

Either metallic Na or NaF were deposited onto Cu(In,Ga)Se$_2$ surfaces and studied by photoelectron spectroscopy and surface photovoltage spectroscopy without breaking the ultra-high vacuum. The deposition of elemental Na at room temperature led to the formation of an intermediate Cu and Ga rich layer at the CIGSe surface, whereas for NaF the composition of the CIGSe surface remained unchanged. A metal like surface induced by an inverted near surface region with a reduced number of defect states was formed after the deposition of Na. Under the chosen experimental conditions, the near surface layer was independent on the amount of Na and stable in time. In contrast, the usage of NaF weakened the inversion and led to an increased band bending compared to the untreated CIGSe sample. The SPV signals decreased with proceeding time after the deposition of NaF.

Keywords: CIGSe, photovoltaic, XPS, SPV, sodium, thin films

a) Email: wolfram.calvet@helmholtz-berlin.de

b) Email: dittrich@helmholtz-berlin.de

c) Current address: EMPA, Überlandstr. 129, CH-8600 Dübendorf, Switzerland

d) Email: iver.lauermann@helmholtz-berlin.de

1. Introduction

Latest improvements of the efficiency of $Cu(In,Ga)Se_2$ (CIGSe) based solar cells up to 22.6 % were related to the post-deposition treatment with alkali metal fluorides such as NaF, KF or RbF [1, 2]. However, the detailed mechanism of these treatments is not yet understood, in spite of numerous activities by our and other groups [3]. Therefore, we have resumed the investigation of the effect of the deposition of alkali metals or their fluorides, starting with Na and NaF on CIGSe using physical vapor deposition (PVD) techniques. Although treatments with either Na metal or NaF have been examined, no previous work has been devoted to a direct comparison of Na and NaF treatments with identical samples in the same UHV system [4-6]. By comparing of both, the Na metal and the fluoride in contact to the absorber, a distinction between the effect of the Na alone and the presence of both Na and F in the CIGSe is possible. Furthermore, the interaction of the valence electron of sodium with the host should become visible when comparing metallic Na as electron donor with ionic Na as electron acceptor.

Therefore, photoelectron spectroscopy (PES) was used in order to investigate the near surface composition by x-ray photoelectron spectroscopy (XPS) and to probe the work function ϕ as well as the valence band maximum E_{VBM} (difference between the valence band edge and the Fermi level) by ultra violet photoelectron spectroscopy (UPS) on both, semiconductor or metal surfaces, respectively [7, 8]. This technique is feasible to monitor changes of the respective parameters upon the stepwise deposition of additional material on the sample. To complement the UPS measurements, modulated surface photovoltage (SPV) spectroscopy in fixed capacitor arrangement [9-11] was applied at the same CIGSe surfaces before and after the deposition of Na or NaF. This method allows to determine qualitatively the degree of charge separation in a device and to measure the band gap of the predominant absorber material. All experiments were performed without breaking the ultra-high vacuum (UHV) at any step.

2. Experiment

Thin CIGSe absorber layers were deposited by co-evaporation from elemental sources (three-stage process) onto soda lime glass substrates coated with Mo [12, 13]. The average composition (surface and bulk) was measured with x-ray fluorescence (XRF) and revealed a Cu-poor regime with a Cu/(Ga+In) ratio (CGI) of 0.95 for sample 1 used for the deposition of Na and 0.85 for sample 2 used for the deposition of NaF. In contrast, the surface composition of both samples determined by XPS (not explicitly shown here) was equal with a CGI ratio of 0.40±0.05 and proves the well-known Cu depletion at the CIGSe surface in accordance to the literature [14, 15]. Therefore, we regard both samples to be identical within the found composition variation. Moreover, the morphology of both samples as measured with secondary electron microscopy (SEM) was similar and revealed the typical micro-crystalline structure and micro-roughness of CIGSe films used for thin film solar cell devices [16]. Before inserting the samples into the UHV system, they were etched with aqueous potassium

cyanide (3 min, KCN 5%), rinsed with deionized water, and then dried under an ultrapure nitrogen gas flow. The UHV based PVD of Na and NaF was realized with a metal dispenser and a water cooled standard effusion cell. Both sources were calibrated with XPS by analyzing the Mo3d and Na1s peak ratio on a Mo coated glass substrate after the successive deposition of Na or NaF. For the experiments, a growth rate of 0.1 nm/min was adjusted and the exposure time was chosen according to a nominal thickness of 0.1 nm for each deposition step as denoted by d_{Na}[Mo] and d_{NaF}[Mo] for Na and NaF, respectively. Throughout the complete growth process, the samples were kept at room temperature (RT). Furthermore, a dedicated UHV chamber for modulated SPV measurements in fixed capacitor arrangement was developed and placed between the preparation and the XPS chamber. The base pressure was below $5 \cdot 10^{-9}$ mbar in both analysis chambers (XPS and SPV) and below $5 \cdot 10^{-10}$ mbar in the preparation chamber (PVD). All units were separated by valves which only were opened for sample transfer from one entity into another. By this in-situ approach, combined XPS, UPS, and SPV measurements were possible without breaking the UHV, thus avoiding uncontrolled contamination and oxidation. As PES facility, a standard laboratory system was used based on a non-monochromatic x-ray source with a Mg anode providing an excitation energy of 1253.6 eV [17]. UPS measurements were done with a standard He lamp, yielding 21.22 eV (HeI) excitation energy. As photoelectron analyser, a standard system with a hemispherical energy filter and an electron detector based on discrete channeltrons was operated at 20 eV pass energy. The angle between x-ray source and entrance cone of the analyser is 54° (magic angle) [18] with the electron lens placed perpendicular to the probed surface. A sputtered Au foil served as reference sample in order to calibrate the energy analyser by making use of the Au4f7/2 transition at 84.0 eV [19]. All measurements were performed at RT. For the analysis, the peaks of interest were fitted by Gaussian-Lorentzian (Voigt) profiles after subtraction of a linear background, yielding intensity I, binding energy position E_B, and line width ΔE of the considered transition. The SPV signals were excited by a halogen lamp that was operated together with a grating monochromator (range 800-1600 nm) and a chopper using a modulation frequency of 7 Hz. The modulated response signals were fed into a high impedance buffer followed by a lock-in amplifier. Therefore, a dedicated chopper with two reference signal channels (in-phase and 90°-phase-shifted) was developed together with a miniaturized double-phase lock-in amplifier and a variable preamplifier integrated into the buffer device.

3. Results and discussion

Figure 1 shows XPS survey spectra of the samples 1 and 2 before and after the deposition of Na and NaF for nominal thicknesses of d_{Na}[Mo] = 0.1 nm and d_{NaF}[Mo] = 0.1 nm. Prior to the Na and NaF deposition, only the substrate related Ga2p, InMNN, Cu2p, In3p, CuLMM, O1s, In3d, SeLMM, C1s, Se3s, SeLMM, Se3p, and Se3d peaks including their spin-orbit split components are present. The measured oxygen and carbon peaks on the bare CIGSe absorbers are small indicating a contamination in the sub-monolayer regime. Since they vanished during the experiment they are neglected in the

following. After the Na or NaF deposition, respectively, additional Na1s, NaKLL F1s, and/or FKLL peaks appear, while the substrate peak intensities related to Cu, In, Ga and Se are weakened due to attenuation effects, which are induced by the thin deposit layer on top of the absorber. The effective thicknesses of deposited Na and NaF were determined by making use of the XPS peak intensities. Assuming a homogenous Na or NaF overlayer, a basic Lambert-Beer formalism was applied in order to analyze the layer formation by using the following equation $I = I_0 \cdot \exp(-\lambda/d)$ with I: measured peak intensity of the respective transition with deposit, I_0: measured peak intensity of the respective transition without deposit, λ: inelastic mean free path of the photoelectrons from the respective transition in the overlayer, and d: theoretical thickness of the deposit layer. Thereby, λ is dependent on the kinetic energy E_{kin} and on the investigated material. It was calculated by the TPP-2M formula using the QUASES program code [20, 21]. Since I and I_0 are experimentally available and λ is theoretically accessible, semi-empirical values for d can be calculated leading to the reduced thicknesses d_{Na} and d_{NaF}.

In Figure 2, Cu 2p3/2 spectra of both samples before and after deposition of metallic Na and NaF for various nominal thicknesses are shown with according fits based on single Voigt profiles pointing to pure Cu states at the surface. Besides weak intensity changes due to damping, strong binding energy variations are primarily visible for metallic sodium as deposit. For the fluoride, the binding energy shift is less significant. The XP spectra of Cu stand exemplarily for Ga, In, and Se that are treated the same way.

In Figure 3, d_{Na} and d_{NaF} are plotted as a function of $d_{Na}[Mo]$ and $d_{NaF}[Mo]$ for the analysis of the different elements of the CIGSe sample. In case of NaF, d_{NaF} increases linearly with $d_{NaF}[Mo]$ for Cu, In, Ga, and Se as indicated by the green straight line which is representative for all elements. The slope of this line is nearly two which is twice as high as expected which means that the reduced layer thickness appears thicker than the nominal one. This could be either explained by a new homogenous phase consisting of further species with an increased thickness or by an overestimated value of λ, which leads to a systematic error. From our experience, a deviation of λ in the range of a factor 2 is unlikely and a lower sticking coefficient of NaF on Mo compared to CIGSe is also not expected since a larger slope means an increased amount of deposited material on top of the CIGSe absorber in comparison to the molybdenum coated glass substrate. Thus, the reaction of NaF with CIGSe forming a new surface phase is most reasonable, keeping in mind that even small changes in the surface composition can have a large impact on the measured XPS intensity.

In case of Na, the dependencies of d_{Na} on $d_{Na}[Mo]$ are different for the observed elements. In case of In and Se, the relationship between d_{Na} and $d_{Na}[Mo]$ is similar to the NaF case, but now with an offset of 0.63 nm. The values of d_{Na} related to Cu are much smaller than for In, Ga, and Se. In addition, the dependency of d_{Na} on $d_{Na}[Mo]$ is not linear anymore and could only be fitted with a quadratic function in a first approximation using a pre-factor of 0.31 nm^{-1} and an offset of 0.02 nm. This trend is also obtained for Ga but now with an additional offset. The course of d_{Na} over $d_{Na}[Mo]$ follows a quadratic

function with a pre-factor of 0.27 nm^{-1} and an offset of 0.57 nm. The qualitative behavior of Ga is similar to that of Cu with an additional offset that is equal to the one used for In and Se. As already mentioned a slope larger than one can be only interpreted by a new layer which was formed upon the reaction of the deposited material with the substrate material that is thicker than the expected nominal layer. However, the found deviations of d_{Na} for the various elements is further explained by thickness dependent changes of the near surface composition of the $Cu(In,Ga)Se_2$ material due to Na-induced migration of Cu and Ga. In this picture, the assumed formalism of a linear attenuation as described by Lambert-Beer's law is not valid anymore because it is based on a homogenous and single layered system. Hence, lower d_{Na} values of Cu and Ga with increasing $d_{Na}[Mo]$ are not interpreted as thinner layers but as higher concentrations within the same volume. Cu is accumulated at the initial CIGSe surface when pure Na is deposited. With ongoing Na deposition, an additional Ga enrichment occurs within the same analysis volume. Besides that it seems that In and Se form a rigid framework where mainly Ga and Cu become mobile in the presence of Na.

The relative shifts ΔE_{peak} of the Cu2p3/2, In3d5/2, Ga2p3/2, and Se3d peaks of samples 1 and 2 before and after deposition of Na or NaF are depicted in Figure 4(a) as a function of $d_{Na}[Mo]$ or $d_{NaF}[Mo]$. Hereby, the peak positions of the bare CIGSe substrates serve as reference. All peaks except those of Cu and Ga, which are related to the Na deposition show the same behaviour of a continuous increase in binding energy with increasing $d_{Na}[Mo]$ and $d_{NaF}[Mo]$ up to $\Delta E_{peak} = 0.3$ eV for $d_{NaF}[Mo] = 0.5$ nm. In contrast, the shifts of the Cu2p3/2 peaks are much larger with values up to $\Delta E_{peak} = 1.00$ eV for $d_{Na}[Mo] = 0.3$ nm. They are only slightly broadened in the range from $\Delta E = 0.65$ to 0.9 eV which is not explicitly shown in the graph. The relatively large shift of the Cu peaks could be explained by the formation of Cu(II), but additional satellite peaks typical for an oxidation state of II are very weak [22]. However, the Cu2p and CuLMM based modified Auger parameter α increases from 1849.3 for the bare absorber to 1850.2 for the Na-treated CIGSe, indicating the transition of Cu(I) to a species that is closer to Cu(II). We assume that surface near copper still exists as Cu(I) after the deposition of elemental sodium, but with a strongly reduced local electron density as indicated by the binding energy shift. A similar behaviour is also found for the Ga2p3/2 peaks with less pronounced relative shifts. The fact that the shift of the remaining peaks follows the nominal thickness more or less linearly is attributed to a downward band bending, which supports the assumption of field induced migration of ionized Cu and Ga species [23, 24]. The valency of Cu that remains in the near surface and Cu-poor host lattice is changed due to the formation of Cu vacancies in the neighborhood that are filled with Na forming Na_{Cu} defects [25]. This induces a local variation of the electron density as well as a distorted lattice, leading to a stronger oxidized Cu atom. In this very simple model the binding state of Na is not clear. XPS data for Na that we obtained (not explicitly shown here) do not reveal any differences between Na and NaF and fit well to the 'unreacted' Na species at about 1072.8 eV according to the literature [26]. Obviously, a more profound explanation requires theoretical

calculations depending on different sites of Cu and Na in the CIGSe lattice under the prerequisite of an unchanged near surface stoichiometry.

In Figures 4b) and c), the values for the valence band maximum $E_{VBM} = E_F - E_V$ and the work function ϕ as derived from UPS measurements are shown as a function of $d_{Na}[Mo]$ and $d_{NaF}[Mo]$. In case of the NaF deposition, the valence band maximum follows E_{VBM} = 0.55, 0.66, 0.64, 0.76, and 1.00 eV for $d_{NaF}[Mo]$ = 0.0, 0.1, 0.2, 0.3, and 0.5 nm, respectively. This means that the CIGSe surface changes from a depleted surface towards a nearly inverted one. For the deposition of Na, E_{VBM} equals nearly zero for all valence band spectra which points to metallic states at the surface pinning it. The work function decreases according to ϕ = 4.78 (no deposit), 4.00, 3.80, 3.47, and 2.86 eV for $d_{NaF}[Mo]$ = 0.1, 0.2, 0.3, and 0.5 nm in case of NaF, whereas it changes only very little for Na (ϕ = 3.32, 3.25, and 3.18eV for $d_{Na}[Mo]$ = 0.1, 0.2, and 0.3 nm) which is in accordance with [27]. For comparison, the work function of bulk Na is ϕ = 2.7 eV [28]. The fact that the value of bulk Na is not reached on CIGSe hints to either an inhomogeneous coverage or partially reacted Na with a value of ϕ below the one of CIGSe [29]. Both, valence band maximum and the work function behave consistently in terms of a negligible band bending considering metallic Na (pinning effect). For NaF, the course of the valence band maximum and the work function is consistent with a downwards band bending but cannot be fully explained by it because the maximum spread of E_{VBM} is with 0.45 eV much smaller than the maximum spread of ϕ with 1.92 eV. The only explanation for this is an additional surface dipole that reduces the value of the work function accordingly. This could be either induced by an additional surface phase or a different termination based on NaF.

Figure 5 shows typical SPV spectra of sample 1 after deposition of Na ($d_{Na}[Mo]$ = 0.3 nm). The sign of the in-phase signals is negative, i.e. photo-generated electrons are separated and move towards the external surface, which is typical for a p-type semiconductor in depletion. The phase-shifted signals are very low in comparison to the in-phase signals because the time-dependent response is much faster than the modulation period. For the deposition of Na, the SPV signals increase from 18 µV to 14 mV, independent of $d_{Na}[Mo]$ and independent of storage time in UHV as it can be seen in the insert of Figure 5. The variation is with three orders of magnitude rather moderate due to metallic states at the surface injecting free electrons into the conduction band. The SPV signal does not change with further deposition of Na and a relatively low value of 14 mV of the modulated SPV signal indicates a strong inversion at the CIGSe surface. For the NaF deposition, the SPV signals increases continuously from 10 µV (no deposit) to 35, 70, 160, and 690 µV after successive deposition of NaF for $d_{NaF}[Mo]$ = 0.1, 0.2, 0.3 and 0.5 nm. The increase of the thickness, which goes along with more and more NaF leads to an increase of the band bending from depletion towards inversion. Nevertheless, it must be mentioned that the SPV signals after the deposition of Na are much larger. Furthermore, the SPV signals decrease after 24 h storage in UHV for the last NaF deposition step on sample 2 ($d_{NaF}[Mo]$ = 0.5 nm). It is well known that CIGSe has defect states close to the conduction and valence band edges leading to exponential tails in the SPV spectra below the band gap. The band gaps, which are obtained from

Tauc-plots of the SPV spectra amount to 1.02 and 1.06 eV for sample 1 and 2, respectively, which is in good agreement to the theoretical value of Ga-poor CIGSe.

Summary

In order to investigate the influence of alkali metals and their fluorides on chalcopyrite absorbers, a comparative study of Na versus NaF on CIGSe was conducted within an in-situ approach using both XPS and SVP, respectively. It turned out that both species show a different behavior in contact to the absorber. In case of pure sodium, diffusion into the bulk material occurs, leading to a partial accumulation of Cu and Ga. The changed chemical environment induces a pronounced shift of the Cu2p line in XPS to higher binding energies while maintaining the oxidation state +1. In addition, metal-like Na states at the CIGSe surface are pinning the band edges accordingly. This is attributed to a Na-induced phase with a work function larger than the one of metallic sodium which points to an intermediate Na species as mentioned in the literature [26], which is unknown so far. The SPV measurements are in agreement with these findings and hint to a strong inversion. In contrast to this, the deposition of NaF leads to a defined overlayer with strongly reduced interdiffusion effects. UPS/XPS data reveal a strong band bending which shows an inverted p-type semiconductor. However, SPV indicates a less pronounced inversion for NaF compared to Na. The electronic properties of the CIGSe surface change linearly with increasing thickness in case of NaF, whereas for elemental Na a step like behavior after the first Na deposition is observed. In both cases the SPV signals are stable over time. In the next step we will compare solar cell performance of devices treated with either Na metal or NaF.

Figure captions

Figure 1: XPS survey spectra of samples 1 and 2 before and after deposition of Na or NaF ($d_{Na}[Mo]$ = $d_{NaF}[Mo]$ = 0.1 nm). The specific Ga2p1/2, Ga2p3/2, InMNN, Na1s, Cu2p1/2, Cu2p3/2, In3p1/2, In3p3/2, CuLMM, O1s, NaKLL, In3d3/2, In3d5/2, SeLMM, C1s, Se3s, SeLMM, Se3p1/2, Se3p3/2 and Se3d3/2,5/2 peaks are marked.

Figure 2: Cu 2p3/2 spectra of samples 1 and 2 before and after deposition of 0.1; 0.2 and 0.3 nm of Na and NaF, respectively. Raw data are marked with symbols (as indicated in the figure), and fits (with Voigt functions) are shown as lines

Figure 3: Dependencies of the reduced thicknesses on the nominal thicknesses of Na (filled symbols) and NaF (open symbols). The reduced thicknesses were obtained by analysis of the Cu2p3/2 (squares), In3d5/2 (circles), Ga2p3/2 (triangles) and Se3d (stars) peaks of samples 1 and 2 before and after deposition of Na or NaF. The solid, dashed and dotted lines represent fits of linear or quadratic functions which are further discussed in the text.

Figure 4: Dependencies of the shifts of the Cu2p3/2 (squares), In3d5/2 (circles), Ga2p3/2 (triangles) and Se3d (stars) peaks (a), of the differences between the Fermi level and the valence band onset (b) and of the work function values (c) of samples 1 and 2 before and after deposition of Na (circles) or NaF (triangles), respectively.

Figure 5: In-phase (filled circles) and 90° phase-shifted (open circles) modulated surface photovoltage spectra of sample 1 after deposition of Na ($d_{Na}[Mo]$ = 0.3 nm). The insert shows the dependency of the absolute in-phase signals at 1000 nm of samples 1 and 2 before and after deposition of Na (filled circles) or NaF (filled triangles). The open circles and triangles correspond to measurements after 24, 48 or 72 h, as indicated.

Figures

Figure 1

Figure 2

Figure 3

11
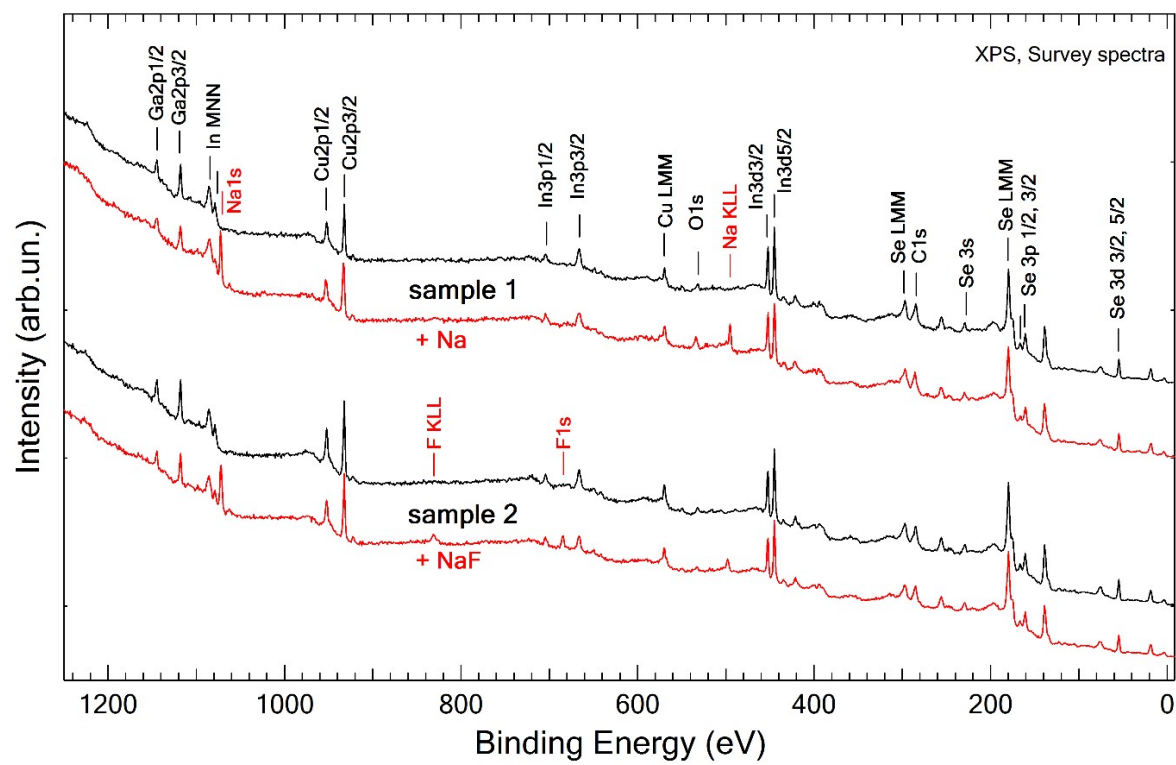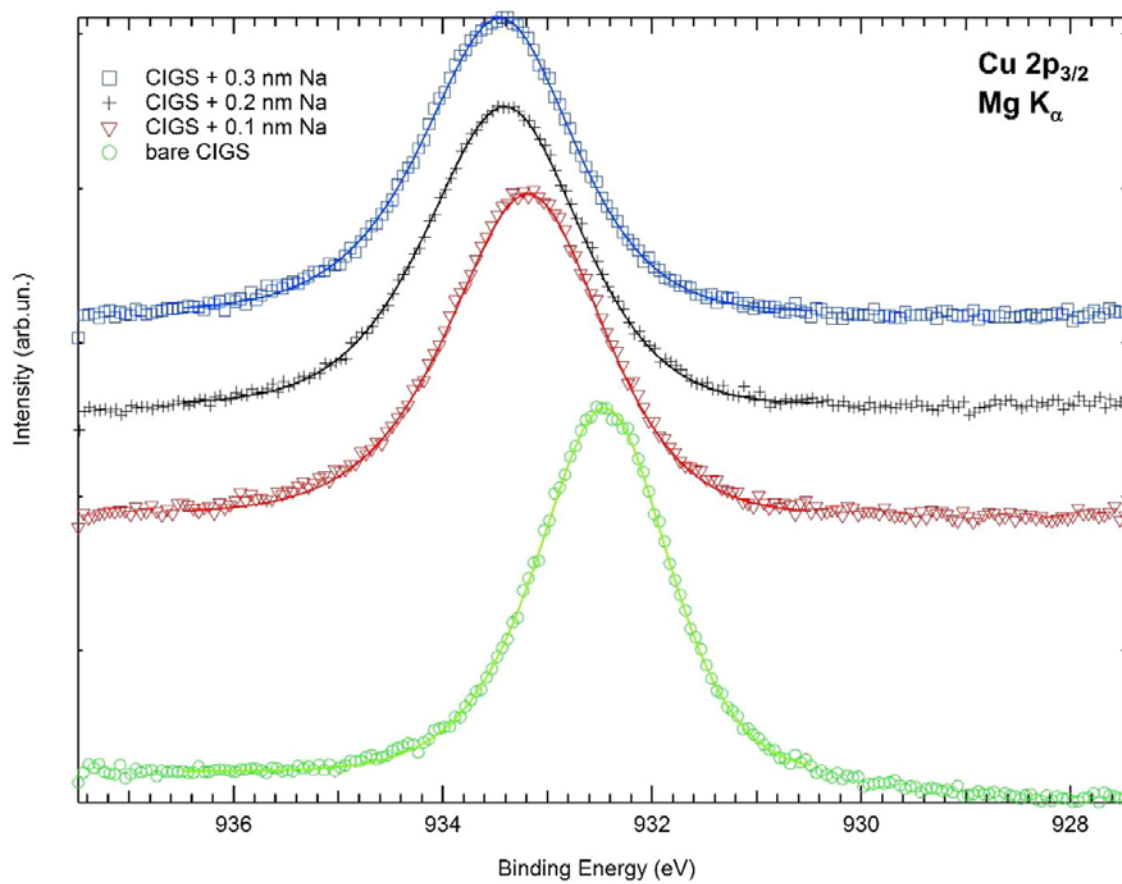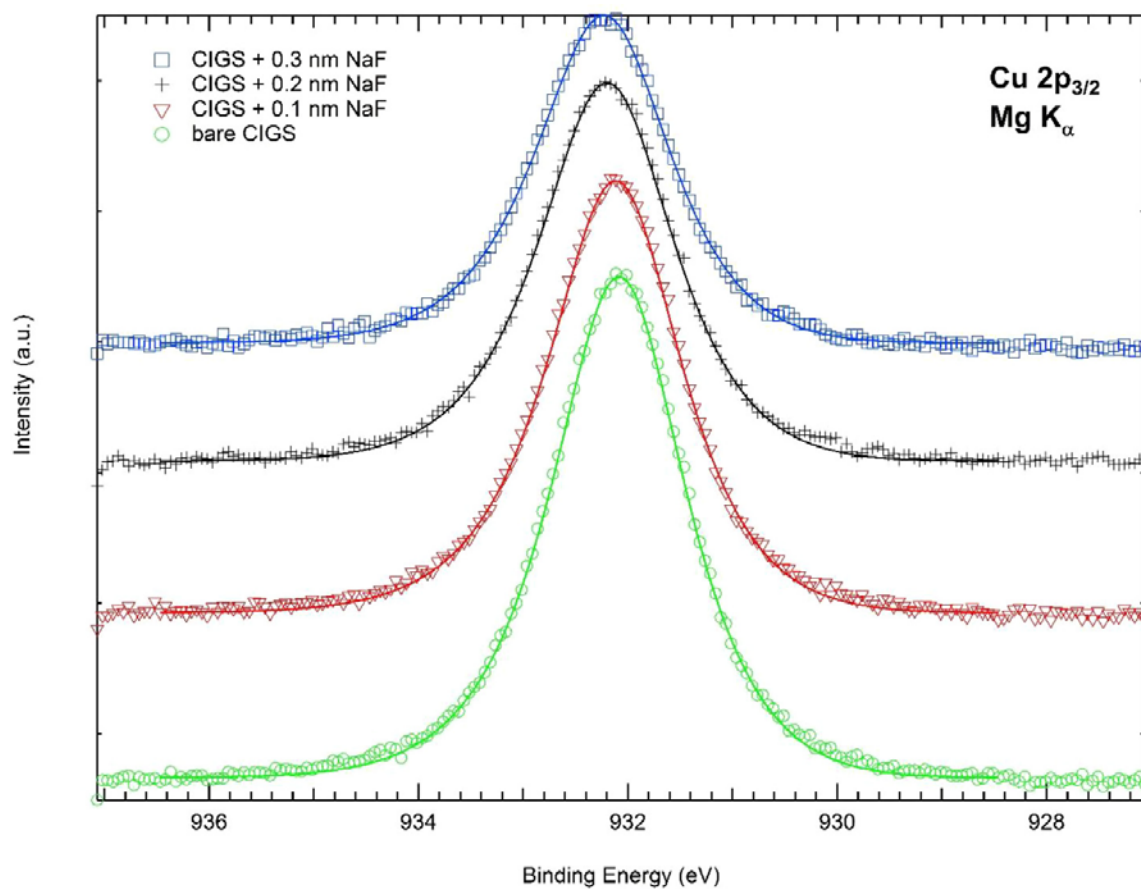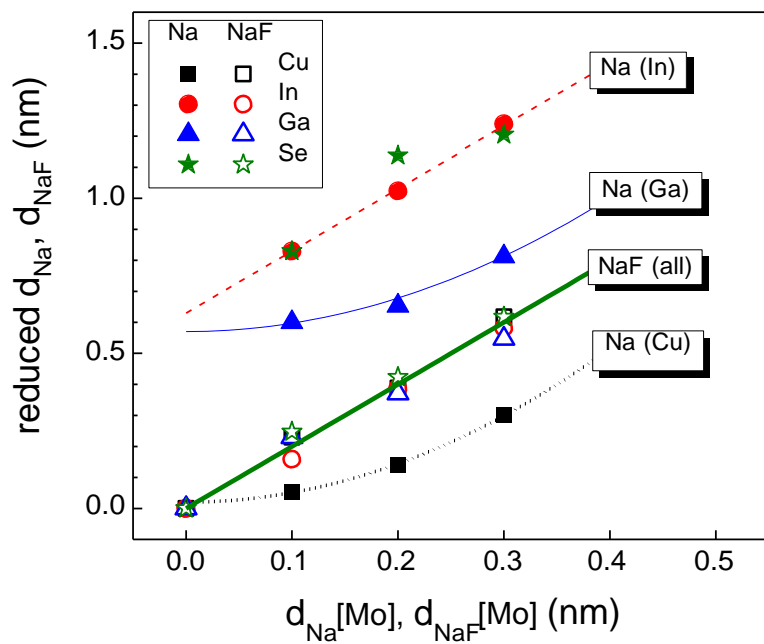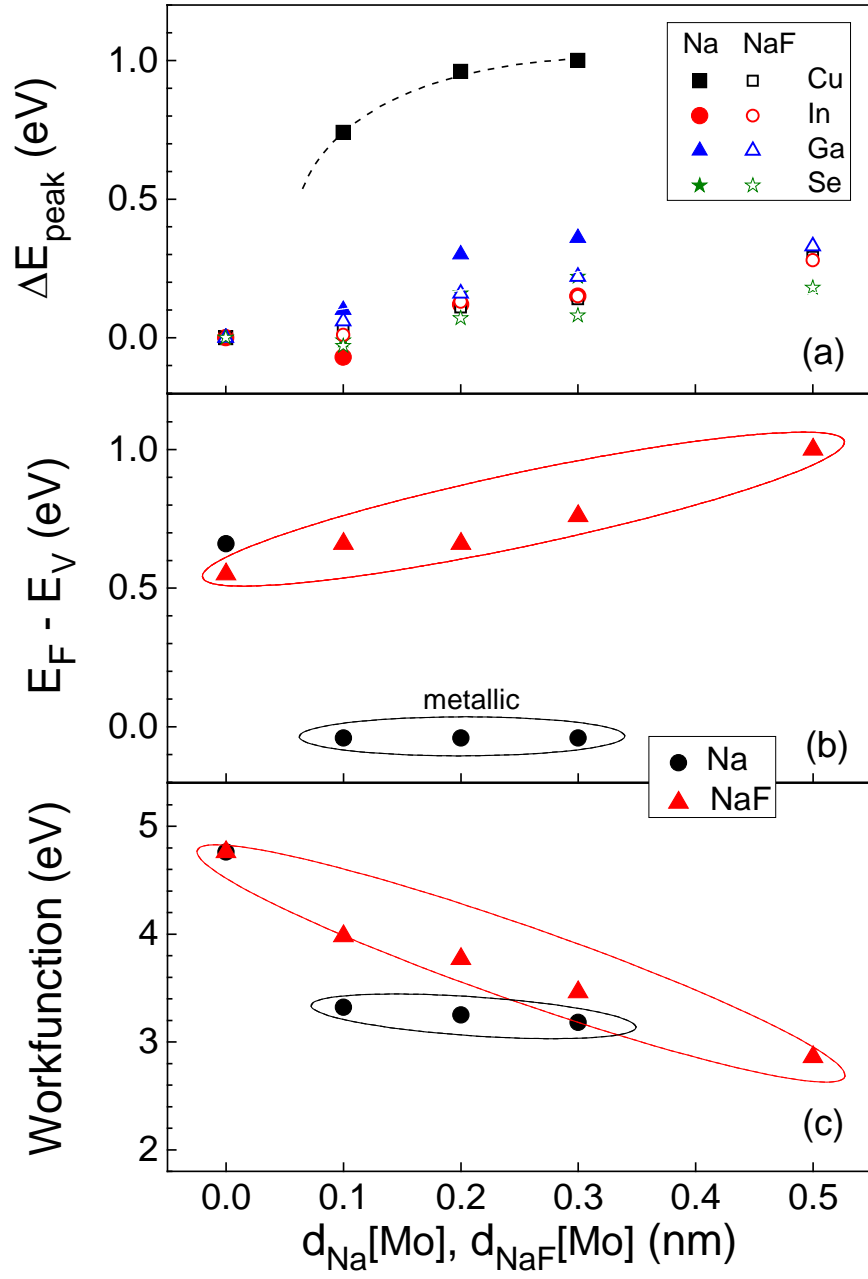
Figure 4

Figure 5
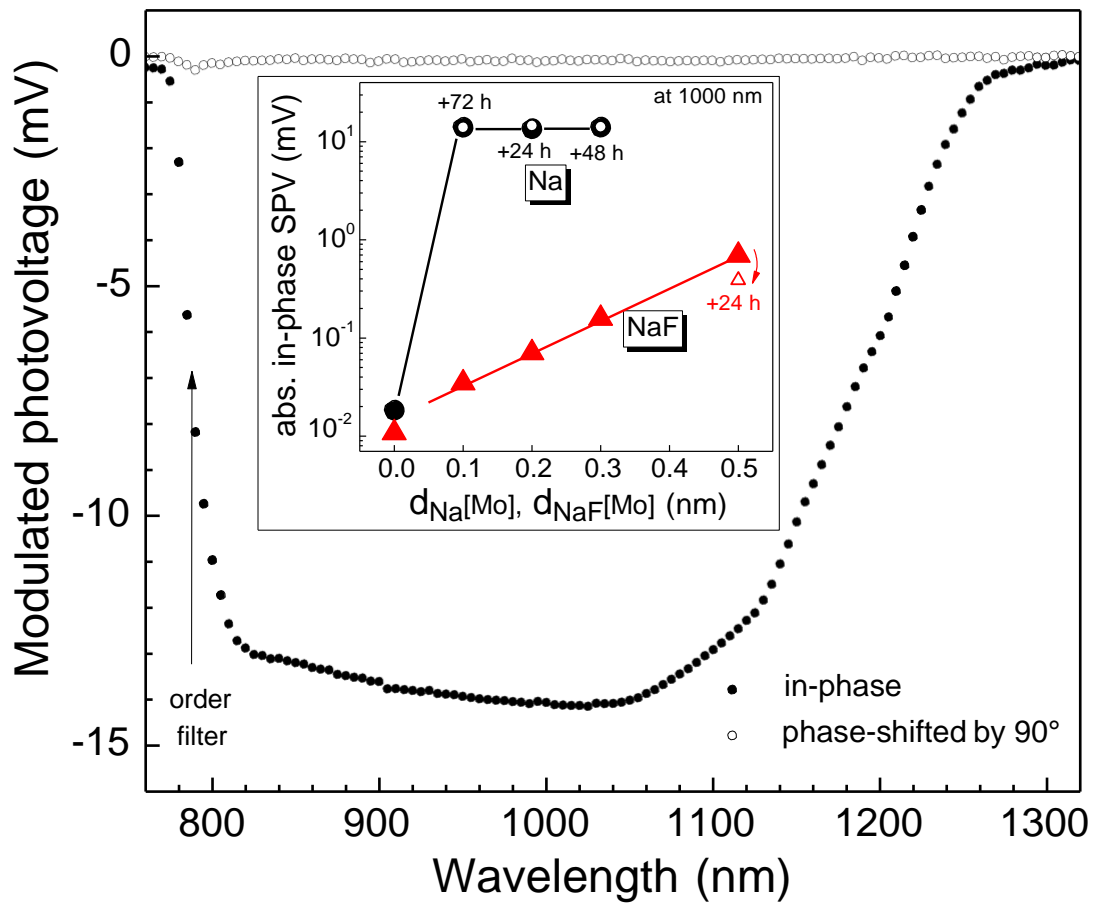
References

[1] P. Jackson, R. Wuerz, D. Hariskos, E. Lotter, W. Witte, M. Powalla, Effects of heavy alkali elements in $Cu(In,Ga)Se_2$ solar cells with efficiencies up to 22.6%, Phys. Status Solidi RRL, 10 (2016) 583-586.

[2] A. Chirila, P. Reinhard, F. Pianezzi, P. Bloesch, A.R. Uhl, C. Fella, L. Kranz, D. Keller, C. Gretener, H. Hagendorfer, D. Jaeger, R. Erni, S. Nishiwaki, S. Buecheler, A.N. Tiwari, Potassium-induced surface modification of $Cu(In,Ga)Se_2$ thin films for high-efficiency solar cells, Nature Mat., (2013).

[3] R. Caballero, M. Nichterwitz, A. Steigert, A. Eicke, I. Lauermann, H.W. Schock, C.A. Kaufmann, Impact of Na on $MoSe_2$ formation at the CIGSe/Mo interface in thin-film solar cells on polyimide foil at low process temperatures, Acta Materialia, 63 (2014) 54-62.

[4] J. Hedstrom, H. Ohlsen, M. Bodegard, A. Kylner, L. Stolt, D. Hariskos, M. Ruckh, H.W. Schock, in: 23rd IEEE Photo. Spec. Conf. (PVSC), Louisville KY, (1993) 364-371.

[5] M. Lammer, U. Klemm, M. Powalla, Sodium co-evaporation for low temperature $Cu(In,Ga)Se_2$ deposition, Thin Solid Films, 387 (2001) 33-36.

[6] M. Lammer, R. Kniese, M. Powalla, In-line deposited $Cu(In,Ga)Se_2$ solar cells: influence of deposition temperature and Na co-evaporation on carrier collection Thin Solid Films, 451-452 (2004) 175-178.

[7] W. Calvet, C. Pettenkofer, H.-J. Lewerenz, Initial phases of $CuInS_2$-Si heteroepitaxy, J. Vac. Sci. Technol. B, 21 (2003) 1335.

[8] W. Calvet, H.-J. Lewerenz, C. Pettenkofer, Model Experiments on Growth Modes and Interface Electronics of $CuInS_2$: Ultrathin Epitaxial Films on GaAs (100) Substrates, Phys. Stat. Sol., A (2014) 1-10.

[9] V. Duzhko, V.Y. Timoshenko, F. Koch, T. Dittrich, Photovoltage in nanocrystalline porous TiO_2, Phys. Rev. B, 64 (2001) 1-7.

[10] T. Dittrich, A. Gonzáles, T. Rada, T. Rissom, E. Zillner, S. Sadewasser, M.C. Lux-Steiner, Comparative study of $Cu(In,Ga)Se_2$/CdS and $Cu(In,Ga)Se_2$/In_2S_3 systems by surface photovoltage techniques, Thin Solid Films, 535 (2013) 357-361.

[11] L. Kronik, Y. Shapira, Surface photovoltage phenomena: theory, experiment, and applications, Surf. Sci. Reports, 37 (1999) 1-206.

[12] C.A. Kaufmann, T. Unold, D. Abou-Ras, J. Bundesmann, A. Neisser, R. Klenk, R. Scheer, K. Sakurai, H.-W. Schock, Investigation of coevaporated $Cu(In,Ga)Se_2$ thin films in highly efficient solar cell devices, Thin Solid Films, 515 (2007) 6217- 6221.

[13] C.A. Kaufmann, A. Neisser, R. Klenk, R. Scheer, Transfer of $Cu(In,Ga)Se_2$ thin film solar cells to flexible substrates using an in situ process control, Thin Solid Films, 480 - 481 (2005) 515-519.

[14] D. Schmid, M. Ruckh, H.W. Schock, Photoemission studies on $Cu(In,Ga)Se_2$ thin films and related binary selenides, Appl. Surf. Sci., 103 (1996) 409.

[15] H. Mönig, C.-H. Fischer, R. Caballero, C.A. Kaufmann, N. Allsop, M. Gorgoi, R. Klenk, H.-W. Schock, S. Lehmann, M.C. Lux-Steiner, I. Lauermann, Surface Cu depletion of $Cu(In,Ga)Se_2$ films: An investigation by hard X-ray photoelectron spectroscopy, Acta Materialia, 57 (2009) 3645-3651.

[16] B. Ümsür, W. Calvet, A. Steigert, I. Lauermann, M. Gorgoi, K. Prietzel, D. Greiner, C.A. Kaufmann, T. Unold, M.C. Lux-Steiner, Investigation of the potassium fluoride post deposition treatment on the CIGSe/CdS interface using hard X-ray photoemission spectroscopy – a comparative study, Phys. Chem. Chem. Phys. , 18 (2016) 14129-14138.

[17] I. Lauermann, A. Steigert, CISSY: A station for preparation and surface/interface analysis of thin film materials and devices JLSRF, 2 (2016) A-67.

[18] P.L.J. Gunter, O.L.J. Gijzeman, J.W. Niemantsverdriet, Surface roughness effects in quantitative XPS: magic angle for determining overlayer thickness, Appl. Surf. Sci., 115 (1997) 342-346.

[19] M.P. Seah, G.C. Smith, M.T. Anthony, AES : Energy Calibration of Electron Spectrometers. I-An Absolute, Traceable Energy Calibration and the Provision of Atomic Reference Line Energies, Surf. & Interf. Anal. , 15 (1990) 293-308.

[20] S. Tougaard, QUASES-IMFP-TPP2M, Version 2.2, http://www.quases.com.

[21] S. Tanuma, C.J. Powell, D.R. Penn, Calculation of electron inelasticmean free paths. V: Data of 14 organic compounds over the 50-2000 eV range., Surf. Interf. Anal., 21 (1993).

[22] J.P. Espinos, J. Morales, A. Barranco, A. Caballero, J.P. Holgado, A.R. Gonzlez-Elipe, Interface Effects for Cu, CuO, and Cu_2O Deposited on SiO_2 and ZrO_2. XPS Determination of the Valence State of Copper in Cu/SiO_2 and Cu/ZrO_2 Catalysts, J. Phys. Chem., B (2002) 6921-6929.

[23] K. Gartsman, L. Chernyak, V. Lyahovitskaya, D. Cahen, V. Didik, V. Kozlovsky, R. Malkovich, E. Skoryatina, V. Usacheva, Direct evidence for diffusion and electromigration of Cu in $CuInSe_2$, J. Appl. Phys., 82 (1997) 4282-4285.

[24] J.F. Guillemoles, The puzzle of $Cu(In,Ga)Se_2$ (CIGS) solar cells stability, Thin Solid Films, 403-404 (2002) 405-409.

[25] S.-H. Wei, S.B. Zhang, A. Zunger, Effects of Na on the electrical and structural properties of $CuInSe_2$, J.Appl. Phys., 85 (1999) 7214.

[26] C. Heske, R. Fink, E. Umbach, W. Riedl, F. Karg, Na-induced effects on the electronic structure and composition of $Cu(In,Ga)Se_2$ thinfilm surfaces, Appl. Phys. Lett., 68 (1996) 3431-3433.

[27] C. Heske, G. Richter, Z. Chen, R. Fink, E. Umbach, W. Riedl, F. Karg, Influence of Na and H_2O on the surface properties of $Cu(In,Ga)Se_2$ thin films, J. Appl. Phys., 82 (1997) 2411-2420.

[28] H.J. Whitefield, J.J. Brady, New Value for Work Function of Sodium and the Observation of Surface-Plasrnon Effects, Phys. Rev. Lett., 26 (1971) 380-383.

[29] S. Siebentritt, U.R. (Eds.), Wide-Gap Chalcopyrites, Springer, Berlin, 2006